Design of two-dimensional apodized grating couplers with Gaussian diffractive mode

Hua Wu (武 华)[1,2], Chong Li (李 冲)[1], Qiaoli Liu (刘巧莉)[1], Bai Liu (刘 白)[1], Jian Dong (董 建)[1], Lei Shi (史 磊)[1], and Xia Guo (郭 霞)[1,*]

[1]*Photonic Device Research Laboratory, College of Electronic Information and Control Engineering, Beijing University of Technology, Beijing 100124, China*

[2]*College of Physics and Electronic Information, Gannan Normal University, Ganzhou 341000, China*

**Corresponding author: guo@bjut.edu.cn*

Received January 21, 2015; accepted March 26, 2015; posted online April 29, 2015

Two-dimensional apodized grating couplers are proposed with grating grooves realized by a series of nanorectangles, with the feasibility of digital tailoring the equivalent refractive index of each groove in order to obtain the Gaussian output diffractive mode in order to enhance the coupling efficiency to the optical fiber. According to the requirement of leakage factor distribution for a Gaussian output profile, the corresponding effective refractive index of the grating groove, duty cycle, and period are designed according to the equivalent medium theory. The peak coupling efficiency of 93.1% at 1550 nm and 3 dB bandwidth of 82 nm are achieved.

OCIS codes: 050.2770, 050.6624, 050.2065.

doi: 10.3788/COL201513.050501.

Grating couplers, which can input and output light between chips and optical fibers, are widely used in the field of silicon photonic integrated circuits[1–3]. Lithographically defined diffraction gratings implemented in a silicon waveguide with no need of cleaving the samples make the wafer-scale testing and large volume fabrication possible[4–7]. The coupling efficiency η of a grating coupler is improved by optimizing the grating structure in recent years, such as by adding a gold bottom mirror to reflect back the downwards light towards the optical fiber due to the poor directionality of the grating couplers[8]. The mode mismatch between the exponentially decreased diffraction field and the Gaussian profile of the optical fiber limits the further improvement of coupling efficiency for the uniform grating couplers, whose periods and duty cycles are the same. The power confined in the uniform gratings decays exponentially according to $P = P_0 \exp(-2\alpha z)$, where P_0 is the input power in the waveguide, z is the light propagation distance along the grating, and α is the leakage factor which determines the profile of the diffraction light[9]. In a uniform grating coupler, the diffractive light power decreases exponentially with the light propagation distance z because α is a constant in the uniform gratings. However, the standard single-mode optical fiber mode is Gaussian profile. The maximum coupling efficiency between a uniform grating coupler and optical fiber is limited to be only about 80% because of mode mismatch[10]. Apodized grating coupler can be used to adjust the leakage factor distribution and thus to improve the mode matching. The apodization has been previously implemented in 1D phase masks for apodized fiber Bragg gratings fabrication[11–13].

Leakage factor α can be tailored by the refractive index of the grating groove and the duty cycle. Tamir[14] found for the negative first-order diffraction, leakage factor $\alpha \propto (n_t^2 - n_g^2)^2 \sin^2(\pi d/\Lambda)$, where n_t and n_g are the refractive index of the grating teeth and groove, respectively; d is the width of the grating teeth; Λ is the period of the grating; d/Λ is the duty cycle. Mathematically, the item $(n_t^2 - n_g^2)$ can change from 0 to $(n_t^2 - 1)$, which corresponds to the shallow etch to fully etch of the grooves. Chen[10] obtained the Gaussian field profile by engineering the duty cycle and then the leakage factor along the light propagation direction. For the transverse electric (TE) mode, the calculated maximum coupling efficiency was 84% at 1550 nm. Zaoui[15] obtained the Gaussian field profile by engineering the duty cycle of the grating coupler with a bottom mirror. The calculated maximum coupling efficiency was 94.2% at 1550 nm with a 1 dB bandwidth of 43 nm for the TE mode. Based on the duty cycle engineering, the nonuniform etching depth of the grating grooves was realized by the lag effect during the reactive ion etching process, which tailored the refractive index of grooves. However, the processing is hard to be fully controlled[16].

Nanostructures have exhibited the feasibility of the effective refractive index digital engineering recently, which relaxes the refractive index limitation by the bulk material. According to the equivalent medium theory, if the period of the nanostructures is small enough to suppress diffraction, the discontinuous nanostructures can act as a homogeneous medium with an equivalent refractive index determined by the duty cycle. The equivalent refractive index n_{eq} is given by Rytov's formulas for the TE mode[17]

$$n_{\mathrm{eq}} = [(1-f)n_{\mathrm{air}}^2 + f n_1^2]^{\frac{1}{2}}, \tag{1}$$

where n_{air} is the refractive index of the air, n_1 is the refractive index of dielectric material, and f is the duty cycle.

Fully etched photonic crystals were employed to engineer the refractive index of each groove to fabricate an

apodized grating coupler on the silicon-on-insulator (SOI) platform[18]. The calculated maximum coupling efficiency was 66% at 1550 nm for the TE mode[19]. By adding a bonded aluminum mirror, the calculated maximum coupling efficiency increased to 91% with a 3 dB bandwidth of 76 nm[20]. 2D fully etched nano-rectangles exhibited the capability of tailoring the effective refractive index of the waveguide from 3.22 to 2.16 with linear variation to form subwavelength gratings (SWGs). The calculated maximum coupling efficiency was 52.5% at 1550 nm with a 3 dB bandwidth of 64 nm for the transverse magnetic (TM) mode[21,22]. By tailoring the refractive index of grooves of grating couplers with fully etched nano-rectangles, SWG groove index was varied linearly from 2.80 to 2.20 along the first 10 grating periods, and followed by 15 periods with SWG index of 2.20. The calculated maximum coupling efficiency was 63.5% at 1550 nm with a 3 dB bandwidth of 66 nm for the TE mode[23].

In this work, a series of nano-rectangles as grating grooves of the grating couplers are proposed to digitally tailoring the effective refractive index of each groove according to the equivalent medium theory and then the output profile of the diffractive light to bridge the gap between the grating coupler and optical fiber. The refractive index distribution of the grooves decreases nonlinearly from 3.40 to 2.35 along the first 20 grating periods, then increases nonlinearly from 2.35 to 3.41 along the following eight grating periods. The coupling efficiency of 93.1% at 1550 nm with 3 dB bandwidth of 82 nm is achieved.

Fig. 1 shows the cross section [Fig. 1(a)] and top view [Fig. 1(b)] of the proposed apodized grating coupler, which can be fabricated on SOI substrate with the 220 nm thick top Si layer. Each groove is composed of a series of nano-rectangles along the y-direction with the equivalent refractive index of $n_{\mathrm{eq},i}$ for the ith period determined by the lateral duty cycle $f_{y,i}$ according to the equivalent medium theory. Then the 2D nano-rectangles can be regarded as a conventional 1D grating structure with alternative refractive index of the $n_{\mathrm{eq},i}$ and n_1, longitudinal period $\Lambda_{z,i}$, and duty cycle f_z, as illustrated in Fig. 1(a). Figure 1(c) shows the dependence of the effective refractive index $n_{\mathrm{eq},i}$ on the duty cycle f_z and corresponding longitudinal period $\Lambda_{z,i}$. The effective refractive index can be tailored in a relatively large range, as shown in Fig. 1(c). Figure 1(d) shows the periodical dependence of the grating directionality as a function of the buried oxide (BOX) thickness. The thickness of the BOX can cause constructive interference between the upward directed diffraction and the reflection at the BOX and the silicon substrate interface. We propose 2200 nm of the thickness of BOX in this work according to Fig. 1(d). In practice, SOI wafers have a standard BOX thickness. The thickness difference can be overcome by modifying the grating radiation angle[23]. In order to increase the directionality of the grating couplers, the mirror is designed on the back of the wafer. All the downward-diffracted light is assumed to be reflected at the perfect gold mirror. For the 1550 nm wavelength, the refractive indices are $n_1 = 3.476$

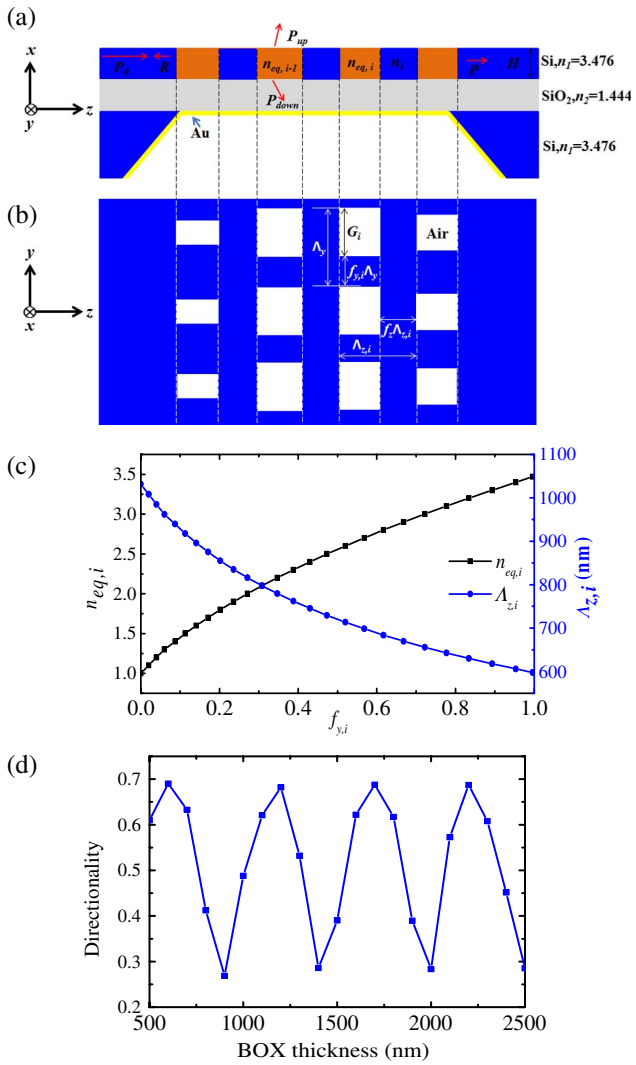

Fig. 1. Schematic of an apodized grating coupler: (a) side view; (b) top view. (c) Relationship of the equivalent refractive index $n_{\mathrm{eq},i}$ and longitudinal grating period $\Lambda_{z,i}$ with the lateral duty cycle $f_{y,i}$. (d) Grating directionality as a function of BOX thickness.

for Si, $n_2 = 1.444$ for SiO_2, and $n_{\mathrm{air}} = 1$ for air. The fiber is tilted 10° with respect to the vertical direction to avoid a large negative second-order Bragg reflection[4].

The average refractive index $n_{\mathrm{eq\_}g,i}$ of the ith period of the grating can be expressed by[24]

$$n_{\mathrm{eq\_}g,i} = (1 - f_z)n_{\mathrm{eq},i} + f_z n_1. \tag{2}$$

The duty cycle in the z direction f_z is fixed to be 0.5 to enhance the diffractive light[14]. Then each equivalent period structure with average refractive index $n_{\mathrm{eq\_}g,i}$ can be regarded as a planar period waveguide layer sandwiched between the index matching gel and the bottom SiO_2[25]. The effective refractive index $n_{\mathrm{eff},i}$ of the ith period waveguide in the grating region can be calculated by using the fundamental TE mode dispersion relation of multilayer planar waveguides[26]

$$(n_{\mathrm{eq\_}g,i}^2 - n_{\mathrm{eff},i}^2)^{1/2}\frac{2\pi}{\lambda}H = \tan^{-1}\left(\frac{n_{\mathrm{eff},i}^2 - n_3^2}{n_{\mathrm{eq\_}g,i}^2 - n_{\mathrm{eff},i}^2}\right)^{1/2} + \tan^{-1}\left(\frac{n_{\mathrm{eff},i}^2 - n_2^2}{n_{\mathrm{eq\_}g,i}^2 - n_{\mathrm{eff},i}^2}\right)^{1/2}, \tag{3}$$

where λ is the center wavelength of 1550 nm, H is the thickness of the Si waveguide layer, and $n_3 = 1.46$ is the refractive index of the index-matching gel. The grating period in the beam propagating direction $\Lambda_{z,i}$ is determined by the phase-matching condition[4]

$$\Lambda_{z,i} = q\lambda/[n_3 * \sin(\theta) - n_{\mathrm{eff},i}], \tag{4}$$

where diffraction order $q = -1$, and $\theta = 10°$. Each period waveguide in the grating region with effective index $n_{\mathrm{eff},i}$ has its corresponding leakage factor according to $\alpha = -\frac{\ln P - \ln P_0}{2z}$ [27].

However, to achieve a Gaussian-shaped output profile, the leakage factor should follow[28]

$$2\alpha(z) = G^2(z)/\left[1 - \int_0^z G^2(t)\mathrm{d}t\right], \tag{5}$$

where $G(z)$ is the normalized Gaussian function. Figure 2 shows the calculation results of the Gaussian function and corresponding leakage factor according to Eq. (5). The leakage factor increases from 0 to 0.45 μm^{-1} when the z value reached to 14 μm, then decreases to 0 within the length of 20 μm. The inset of Fig. 2 is the calculation result of the relationship of α_i with $f_{y,i}$, which shows that α_i increases from 0.366 to 0.497 μm^{-1} with $f_{y,i}$ from 0 to 0.568. Then α_i decreases rapidly to zero if further increasing the duty cycle of the groove $f_{y,i}$.

Combined with the calculation results of Fig. 1(c) and Fig. 2, and assuming $\Lambda_y = 450$ nm, that is, satisfying the equivalent medium theory, the values of $f_{y,i}$, $n_{\mathrm{eq},i}$ and $\Lambda_{z,i}$ of each period are selected, as shown in Fig. 3. The distribution of the nano-rectangles presents asymmetric. The

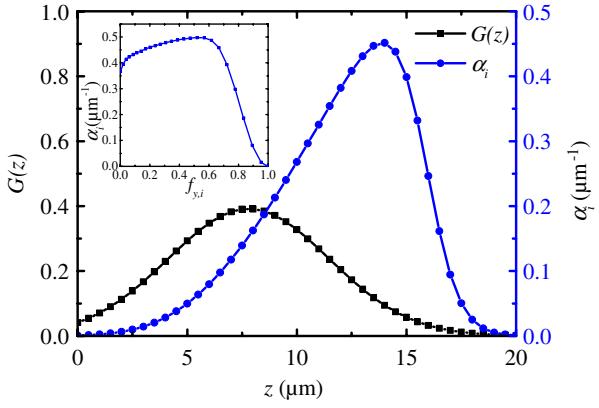

Fig. 2. Calculation results of the Gaussian function and the corresponding leakage factor distribution. Inset, relationship of the leakage factor α_i with the duty cycle of the groove $f_{y,i}$.

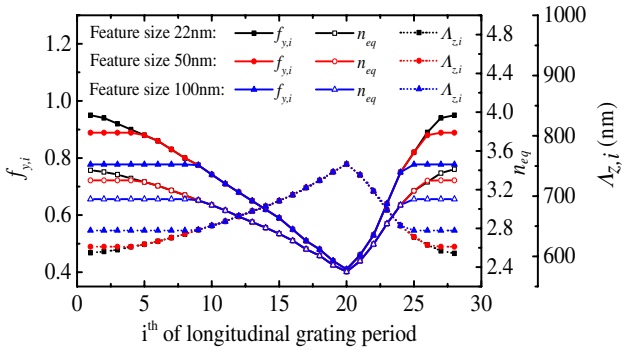

Fig. 3. Value distribution along the longitudinal grating period number of duty cycle of the ith groove $f_{y,i}$, equivalent refractive index $n_{\mathrm{eq},i}$ of the grating grooves, and longitudinal grating period $\Lambda_{z,i}$ for apodized grating couplers.

largest nano-rectangle is in the middle of the grating with the $f_{y,i}$ of 0.41 at the 20th longitudinal grating period. The feature size is 22 nm which locates at the both sides of the grating. The behavior of $n_{\mathrm{eq},i}$, $n_{\mathrm{eq\_}g,I}$, and $n_{\mathrm{eff},i}$ are similar with $f_{y,i}$ according to Eq. (1)–(3) and only the relationship of $n_{\mathrm{eq},i}$ with the grating period is presented for simplicity.

The Eigenmode expansion technique[29] with the perfect matched layer-absorbing boundary condition[30] is utilized to calculate the electric field distribution of the proposed grating couplers. A Gaussian profile with a full width $(1/e)$ of 10.4 μm is used as a model for the optical fiber mode. The Gaussian beam approximation is very accurate for calculating the launching efficiency at the input of a fiber[31]. For the beam diameter, we use 10.4 μm at wavelength 1550 nm, because this value is given in the data sheet of the fibers (Corning SMF-28). This beam diameter is in fact also wavelength-dependent, but we neglect this in our calculations to simplify the calculations. In order to eliminate the fiber's facet reflection, a layer of index-matching gel with a refractive index similar to that of SiO_2 is assumed to fill up the space between the fiber and the grating coupler[16].

Figure 4(a) shows the coupling efficiency of the proposed apodized grating couplers with gold layer as the bottom mirror in the wavelength range from 1500 to 1600 nm. The simulated maximum coupling efficiency of apodized grating couplers to the optical fiber is 93.1% at 1550 nm with 3 dB bandwidth of 82 nm. Compared with the upward diffraction efficiency of 95.6% before coupling to the optical fiber, the mode matching degree is 97.3%, which demonstrates better Gaussian mode matching. Figure 4(b) presents the calculation result of the electric field distribution at the wavelength of 1550 nm when the light propagates in the grating couplers. The equiphase surface, illustrated by the alternative color as shown in Fig. 4(b), shows the wave propagation performance. The angle θ of the upward-diffracted wave relative to the vertical direction is measured to be 10°, which agrees with our design. Different from the exponentially decaying field profile diffracted from a uniform grating, the profile of the electric field intensity of the upward-diffracted wave

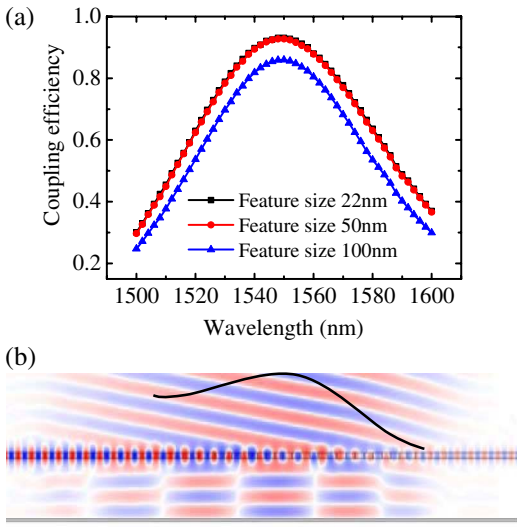

Fig. 4. (a) Coupling efficiency versus wavelength of the apodized grating couplers in three feature sizes; (b) electric field intensity distribution when the light propagates in the grating couplers with gold bottom mirror at the wavelength of 1550 nm.

follows the Gaussian distribution, as illustrated by the color depth in Fig. 4(b). The Gaussian profile of the diffraction field is beneficial to the coupling efficiency improvement between the grating coupler and optical fiber.

In practice, the small feature size makes the difficulties in nano-structure fabrication. To evaluate the effect of the feature size, the calculated coupling efficiency of the apodized grating couplers with the minimum size of 50 and 100 nm are also presented in Fig. 4(a). The maximum coupling efficiency decreases to be 92.7 and 85.9% with 3 dB bandwidth of 81 and 74 nm, respectively. The decrease of the coupling efficiency is caused by the mode mismatch due to the relatively large change of leakage factors.

In conclusion, a structure of 2D apodized grating coupler is proposed which utilizes a series of nano-rectangles as grating grooves of the grating couplers to digitally tailoring the effective refractive index of each groove, which is beneficial to modulate the diffraction profile to a Gaussian field profile of the upward-diffracted light. The peak coupling efficiency of 93.1% at 1550 nm with 3 dB bandwidth of 82 nm is achieved. The matching degree is 97.3% between the field profile of upward-diffracted light and optical fiber mode, which improves the coupling efficiency of the grating couplers by mode matching technique.

This work was supported by the National Natural Science Foundation of China (Nos. 61222501 and 61335004) and the Specialized Research Fund for the Doctoral Program of Higher Education of China (No. 20111103110019).

References

1. T. Baehr-Jones, T. Pinguet, P. L. Guo-Qiang, S. Danziger, D. Prather, and M. Hochberg, Nat. Photonics **6**, 206 (2012).
2. D. X. Xu, J. H. Schmid, G. T. Reed, G. Z. Mashanovich, D. J. Thomson, M. Nedeljkovic, X. Chen, D. V. Thourhout, S. Keyvaninia, and S. K. Selvaraja, IEEE J. Sel. Top. Quantum Electron. **20**, 8100217 (2014).
3. P. D. Dobbelaere, in *18th Asia and South Pacific Design Automation Conference* 644 (2013).
4. G. Roelkens, D. Vermeulen, S. Selvaraja, R. Halir, W. Bogaerts, and D. V. Thourhout, IEEE J. Sel. Top. Quantum Electron. **17**, 571 (2011).
5. J. Hu, Y. Huang, X. Ren, X. Duan, Y. Li, and Y. Luo, Chin. Opt. Lett. **12**, 072301 (2014).
6. T. Ma, X. Yuan, W. Ye, W. Xu, S. Qin, and Z. Zhu, Chin. Opt. Lett. **12**, 020501 (2014).
7. C. Ma, Y. Huang, X. Duan, and X. Ren, Chin. Opt. Lett. **12**, 120501 (2014).
8. W. S. Zaoui, M. F. Rosa, W. Vogel, M. Berroth, J. Butschke, and F. Letzkus, Opt. Express **20**, B238 (2012).
9. C. Li, H. J. Zhang, M. B. Yu, and G. Q. Lo, Opt. Express **21**, 7868 (2013).
10. X. Chen, C. Li, C. K. Y. Fung, S. M. G. Lo, and H. K. Tsang, IEEE Photon. Technol. Lett. **22**, 1156 (2010).
11. T. Osuch and Z. Jaroszewicz, Opt. Commun. **284**, 567 (2011).
12. T. Osuch, A. Kowalik, Z. Jaroszewicz, and M. Sarzyński, Appl. Opt. **50**, 5977 (2011).
13. J. Albert, K. O. Hill, B. Malo, S. Thériault, F. Bilodeau, D. C. Johnson, and L. E. Erickson, Electron. Lett. **31**, 222 (1995).
14. T. Tamir and S. T. Peng, Appl. Phys. **14**, 235 (1977).
15. W. S. Zaoui, A. Kunze, W. Vogel, M. Berroth, J. Butschke, F. Letzkus, and J. Burghartz, Opt. Express **22**, 1277 (2014).
16. Y. B. Tang, Z. C. Wang, L. Wosinski, U. Westergren, and S. L. He, Opt. Lett. **35**, 1290 (2010).
17. S. M. Rytov, Sov. Phys. JETP **2**, 466 (1956).
18. L. Liu, M. Pu, K. Yvind, and J. M. Hvam, Appl. Phys. Lett. **96**, 051126 (2010).
19. Y. H. Ding, H. Y. Ou, and C. Peucheret, Opt. Lett. **38**, 2732 (2013).
20. Y. H. Ding, C. Peucheret, H. Y. Ou, and K. Yvind, Opt. Lett. **39**, 5348 (2014).
21. R. Halir, P. Cheben, S. Janz, D. X. Xu, Í. Molina-Fernández, and J. G. Wangüemert-Pérez, Opt. Lett. **34**, 1408 (2009).
22. R. Halir, P. Cheben, J. H. Schmid, R. Ma, D. Bedard, S. Janz, D. X. Xu, A. Densmore, J. Lapointe, and Í. Molina-Fernández, Opt. Lett. **35**, 3243 (2010).
23. D. Benedikovic, P. Cheben, J. H. Schmid, D. X. Xu, L. Jean, S. R. Wang, R. Halir, A. Ortega-Monux, S. Janz, and D. Milan, Laser Photon. Rev. **8**, L93 (2014).
24. X. Chen and H. K. Tsang, IEEE Photon. J. **1**, 184 (2009).
25. S. Peng and G. M. Morris, Opt. Lett. **21**, 549 (1996).
26. D. S. Gao and Z. P. Zhou, Appl. Phys. Lett. **88**, 163105 (2006).
27. D. Taillaert, "Grating couplers as interface between optical fibres and nanophotonic waveguides," Ph.D. Thesis (Ghent University, 2004).
28. D. Taillaert, P. Bienstman, and R. Baets, Opt. Lett. **29**, 2749 (2004).
29. D. F. G. Gallagher and T. P. Felici, Proc. SPIE **4987**, 69 (2003).
30. P. Bienstman, H. Derudder, R. Baets, F. Olyslager, and D. D. Zutter, IEEE Trans. Microwave Theory Technol. **49**, 349 (2001).
31. E. G. Neumann, *Single-Mode Fbers–Fundamentals* (Springer, 1988).